

CHEM MED CHEM

CHEMISTRY ENABLING DRUG DISCOVERY

Accepted Article

Title: Improving the Potency of Cancer Immunotherapy by Dual Targeting IDO1 and DNA

Authors: kun Fang, Guoqiang Dong, Hongyu Wang, Shipeng He, Shanchao Wu, Wei Wang, and Chunquan Sheng

This manuscript has been accepted after peer review and appears as an Accepted Article online prior to editing, proofing, and formal publication of the final Version of Record (VoR). This work is currently citable by using the Digital Object Identifier (DOI) given below. The VoR will be published online in Early View as soon as possible and may be different to this Accepted Article as a result of editing. Readers should obtain the VoR from the journal website shown below when it is published to ensure accuracy of information. The authors are responsible for the content of this Accepted Article.

To be cited as: *ChemMedChem* 10.1002/cmdc.201700666

Link to VoR: <http://dx.doi.org/10.1002/cmdc.201700666>

WILEY-VCH

www.chemmedchem.org

A Journal of



Improving the Potency of Cancer Immunotherapy by Dual Targeting IDO1 and DNA

Kun Fang,^{†[a][b]} Guoqiang Dong,^{†[b]} Hongyu Wang,^[b] Shipeng He,^[a] Shanchao Wu,^[b] Wei Wang,^{*[a][c]} and Chunquan Sheng^{*[b]}

[a] Dr. K. Fang, S. He and Prof. Dr. W. Wang
School of Pharmacy, East China University of Science and Technology
Shanghai 200237, P. R. China.

E-mail: wwang@unm.edu

[b] G. Dong, H. Wang, S. Wu, and Prof. Dr. C. Sheng
Department of Medicinal Chemistry, School of Pharmacy, Second Military Medical University
325 Guohe Road, Shanghai 200433, P. R. China
E-mail: shengcq@smmu.edu.cn

[c] Prof. Dr. W. Wang
Department of Chemistry and Chemical Biology, University of New Mexico
Albuquerque, NM87131-0001, USA

† Dr. K. Fang and G. Dong contributed equally to this work.

Supporting information for this article is given via a link at the end of the document.

Abstract: Here we report the first effort on exploration of the dual-targeting drug design strategy to improve the efficacy of small molecule cancer immunotherapy. New hybrids of IDO1 (indoleamine 2, 3-dioxygenase 1) inhibitors and DNA alkylating nitrogen mustards targeting respective IDO1 and DNA are rationally designed. As the first-in-class example of such molecules, they exhibited significantly enhanced anticancer activity *in vitro* and *in vivo* with low toxicity. The proof-of-concept by the studies has established a critical step toward developing novel and effective immunotherapy for the treatment of cancers.

Cancer immunotherapy by the use of the immune system to treat cancer has been recognized as a pillar of cancer therapy by joining the ranks of surgery, radiation, chemotherapy, and targeted therapy.^[1] However, the overarching challenge in current clinically used immunotherapy is that it is only effective for a fraction of cancer patients whose immunogenic tumor microenvironment can respond to activated immune cells.^[1-2] This is largely because tumor cells are capable of escaping immune surveillance and suppress antitumor immunity.^[3] Among them, kynurenine (Kyn) pathway of tryptophan (Trp) catabolism plays a key role in immune escape,^[4] in which indoleamine 2,3-dioxygenase 1 (IDO1) catalyzes the first and rate-limiting step.^[5] IDO1 is a heme-containing enzyme that oxidizes Trp to *N*-formylkynurenine (NFK) and subsequent deformylation by formamidase produces Kyn.^[6] Both Trp degradation and Kyn accumulation are associated with immune tolerance by affecting T cell activity and altering the tumor microenvironment.^[7] IDO1 has become an attractive target for cancer immunotherapy. Currently, three small molecule IDO1 inhibitors are under clinical development (Figure S1): indoximod (1-D-MT), epacadostat (INCB024360) and GDC-0919.^[8] However, indoximod is a weak IDO1 inhibitor with the IC₅₀ value greater than 100 μM.^[9] GDC-0919 demonstrated a high dose tolerance, but failed to induce tumor eradication and prevent disease progression in phase I clinical trial.^[8c] Hydroxyamidine IDO1 inhibitor epacadostat is still in active clinical development.^[10] Mechanistically, IDO1 inhibitors do not destroy tumor cells directly. A number of studies showed that IDO1-blockade

synergized with traditional chemo-therapeutics to enhance antitumor efficacy both *in vitro* and *in vivo*.^[11] IDO1 inhibitors in combination with cytotoxic chemotherapeutic agents have been identified as an effective remedy in cancer therapy. Moreover, synergistic antitumor effects are observed in combination IDO1 inhibitors with temozolomide or cyclophosphamide.^[11b, 11c] Several clinical trials are underway to determine the potential synergistic effects combining indoximod or epacadostat with traditional cancer chemotherapies.^[10, 12]

Classic DNA alkylating agents (Figure S1) such as nitrogen mustards are widely used clinically for the treatment of a variety of cancers.^[13] However, the poor drug potency, dose-limiting toxicities, drug resistance, substantial pharmacokinetic and response variability remain significant hurdles in the use of these drugs. The search of highly potent and safe DNA alkylation agents represents a long-standing interest in drug discovery.

Although studies have showed that the co-administration of IDO1 inhibitors indoximod or epacadostat with traditional cancer chemotherapies exhibits promising anti-cancer synergistic effects, the simple combination of IDO1 inhibitors indoximod or epacadostat with traditional cancer chemotherapies cannot overcome severe side effects caused by these highly toxic compounds and possible drug-drug interactions. In addition, the different pharmacokinetics, bio-distributions and metabolisms of two individual drugs make them difficult to achieve optimal therapeutic effects, particularly synergistic actions. Ideally, one drug entity with the capacity of targeting two targets simultaneously may overcome these inherently challenging problems. Toward this end, herein we rationally designed new hybrid molecules by incorporation of the pharmacophores of IDO1 inhibitors and DNA alkylating agents. We found that they exhibited highly inhibitory activity against IDO1 with significantly reduced side effects caused by the cytotoxic alkylating agents.

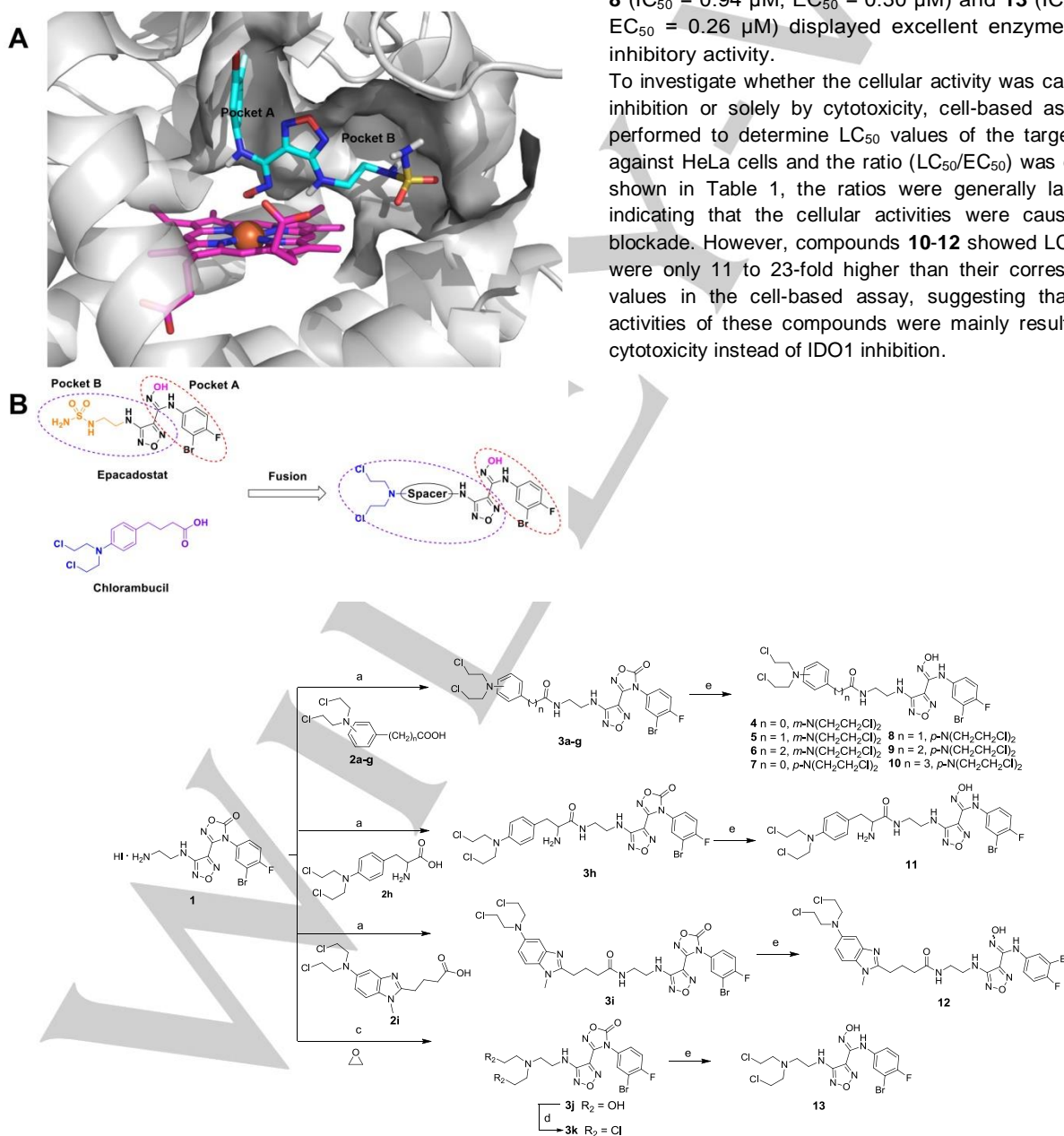
We chose IDO1 inhibitor epacadostat and DNA alkylating agents^[14] chlorambucil and melphalan as the starting points in

the design of dual targeting molecules (Figure 1). Human IDO1 contains a binding pocket in the distal heme site (pocket A) and a second pocket toward the entrance of the active site (pocket B, Figure 1A). Molecular docking was performed to investigate the binding mode of epacadostat with IDO1 (Figure 1A).^[15] The *meta*-bromophenyl, hydroxyamidine and oxadiazole groups in epacadostat are essential for the IDO1 inhibition.^[16] The phenyl and hydroxyamidine groups are bound to the pocket A in the active site of IDO1. The side chain projected out of the active site in pocket B toward solvent, which could be modified to optimize IDO1 inhibitory activity and physicochemical properties. Guided by the binding mode, the aminoethyl-sulfamide substituent of epacadostat is replaced by the alkylating pharmacophore *N,N*-bis(2-chloroethyl)-amine using the pharmacophore fusion strategy. As a result, novel dual targeting molecules **4-13** are rationally designed (Figure 1B), in which various spacers will be investigated to probe IDO1 inhibitory activity and antitumor potency.

Figure 1. (A) Model of epacadostat bound to IDO1 (PDB ID: 4PK5). (B) Design strategy of the dual targeting agents.

The newly designed dual targeting molecules are synthesized using the methods depicted in Scheme 1. The IDO1 inhibitory activity of the synthesized compounds **4-13** was investigated against human recombinant IDO1 and IDO1 in HeLa cells accordingly.^[16] As shown in Table 1, most compounds showed moderate to good activity at the molecular and cellular level. For the compounds conjugated with chlorambucil or phenyl carboxylic acid mustard, *N,N*-bis(2-chloroethyl)-amine group at *meta*-position (compounds **4, 5** and **6**) resulted in better enzyme inhibition than those of the corresponding *para*-position derivatives (compounds **7, 8** and **9**). Moreover, it was observed that the cellular activity was decreased with the increasing of the carbon chain length with the exception of compound **10**. In particular, compounds **4** ($IC_{50} = 0.13 \mu\text{M}$, $EC_{50} = 0.27 \mu\text{M}$), **8** ($IC_{50} = 0.94 \mu\text{M}$, $EC_{50} = 0.30 \mu\text{M}$) and **13** ($IC_{50} = 0.94 \mu\text{M}$, $EC_{50} = 0.26 \mu\text{M}$) displayed excellent enzyme and cellular inhibitory activity.

To investigate whether the cellular activity was caused by IDO1 inhibition or solely by cytotoxicity, cell-based assay was also performed to determine LC_{50} values of the target compounds against HeLa cells and the ratio (LC_{50}/EC_{50}) was calculated. As shown in Table 1, the ratios were generally larger than 30, indicating that the cellular activities were caused by IDO1-blockade. However, compounds **10-12** showed LC_{50} values that were only 11 to 23-fold higher than their corresponding EC_{50} values in the cell-based assay, suggesting that the cellular activities of these compounds were mainly resulted from their cytotoxicity instead of IDO1 inhibition.



Scheme 1. Synthesis of Compounds 4-13. Reagents and Conditions: (a) HATU, DIPEA, DMF, rt, 12 h, yield 42-66%; (b) CF₃COOH, DCM, 40 °C, 3 h, yield 74%; (c) Ethylene oxide, MeOH, 50 °C, overnight, yield 78%; (d) SOCl₂, DCM, 40 °C, 3 h, yield 85%; (e) NaOH, MeOH, rt, 2 h, yield 54-93%.

Table 1. IDO1 enzyme inhibition and cellular potency of target compounds^a.

Compounds	rhIDO1 IC ₅₀ (μM) or %Inhibition at 1 μM	HeLa (EC ₅₀ , μM)	HeLa (LC ₅₀ , μM)	Ratio LC ₅₀ / EC ₅₀
Epacadostat	0.066 ± 0.008	0.029 ± 0.005	>100	>100
4	0.13 ± 0.02	0.27 ± 0.059	39 ± 4.33	>100
5	0.83 ± 0.007	0.47 ± 0.052	52 ± 5.25	>100
6	0.85 ± 0.005	0.86 ± 0.080	54 ± 2.21	63
7	26%	0.21 ± 0.034	32 ± 1.22	>100
8	0.94 ± 0.01	0.30 ± 0.076	27 ± 2.46	91
9	31%	0.86 ± 0.073	27 ± 3.21	32
10	23%	0.79 ± 0.068	18 ± 1.63	23
11	1.3 ± 0.05	1.5 ± 0.15	21 ± 0.54	14
12	10%	2.3 ± 0.13	25 ± 0.87	11
13	0.94 ± 0.02	0.26 ± 0.016	27 ± 1.22	>100

^aIC₅₀, EC₅₀ and LC₅₀ values are the mean of at least three independent assays, presented as mean ± SD.

The target compounds were further screened for their *in vitro* antiproliferative activities against four cancer cell lines (murine colon adenocarcinoma CT-26 cells, human lung cancer A549 cells, colon cancer HCT116 and HT-29 cells) by the standard CCK-8 methods (Table S1). The IC₅₀ values revealed that all compounds showed better antiproliferative activities than positive DNA alkylating drug chlorambucil for all the tested cell lines whereas IDO1 inhibitor epacadostat was totally inactive. All the target compounds exhibited moderate to good antiproliferative potencies with a broad spectrum against all the four cell lines. Finally, compounds 4 and 8 were chosen for the further study because of their potent IDO1 inhibitory activity, highly cellular potency (Figure S2) and moderate *in vitro* cytotoxicity.

To clarify whether compounds 4 and 8 can lead to cell death by apoptosis, an annexin V/FITC/propidium iodide (PI) binding assay was performed. CT-26 cells were treated with vehicle alone or various concentrations of the tested compounds for 48 h, then stained with Annexin V-FITC and PI, and analyzed by flow cytometry. Compounds 4 and 8 generated significant induction of apoptosis in the CT-26 cell line in a dose-dependent manner (Figure S3). The percentage of apoptotic cells for compounds 4 (at 50 μM) and 8 (at 40 μM) were 68.69% and 91.04%, respectively. Therefore, it is concluded that the antiproliferative activity of compounds 4 and 8 could be ascribed to the induction of apoptosis in CT-26 cells.

Cell cycle distribution of compounds 4 and 8 were further examined in CT-26 cells (Figure S4) to investigate whether the cell growth suppression was induced by cell cycle arrest. CT-26 cells were treated with vehicle alone or the tested compounds (compound 4 at 25 μM, compound 8 at 15 μM) for 12 h, 36 h and 48 h, respectively. Initially, both compounds 4 and 8 induced an increase in cells at G2/M phase after 12 h of the drug administration. The results showed a steady increase in cells at G2/M phase in a time-

dependent manner. After exposed with compounds 4 and 8 for 48 h, the ratios in G2/M phase of the cell cycle were 29.23% and 69.72%, respectively. In contrast, the ratio of cells with vehicle in G2/M phase of the cell cycle was 10.24%. The data suggested that the CT-26 cells treated with compound 4 or 8 showed G2/M phase arrest.

In vivo antitumor efficacy of compounds 4 and 8 were firstly evaluated in a CT-26 tumor growth model in immunocompetent mice by measuring tumor growth inhibition (TGI). When implanted tumors had reached a volume of about 100 mm³, compounds 4 and 8 were administered orally (po) at 100 mg/kg twice a day for 14 consecutive days. Epacadostat (100 mg/kg, po, bid) was used as the positive control. As shown in Figure 2A, both compounds 4 and 8 produced significant antitumor activity ($P < 0.001$) with dramatic reduction in tumor growth. Compound 8 showed comparable antitumor activity (TGI = 47.9%) to that of epacadostat (TGI = 47.5%). Notably, compound 4 displayed superior antitumor activity (TGI = 58.2%). Importantly, mice treated with a high dose of 4 and 8 (100 mg/kg, po, bid) showed no significant body weight loss (Figure S5) and no adverse effects were observed. Furthermore, compound 4 was also evaluated for *in vivo* efficacy of tumor xenograft in nude mice bearing human CT-26 tumors. As shown in Figure 2B, it exhibited significant antitumor activity ($P < 0.01$) and reduced 28.6% of the tumor volume. On the basis of the *in vivo* antitumor activity in immunocompetent and immunodeficient mice, it could be reached that the antitumor effect of compound 4 resulted from the synergistic effect of antitumor immunity and cytotoxicity to the tumor cell.

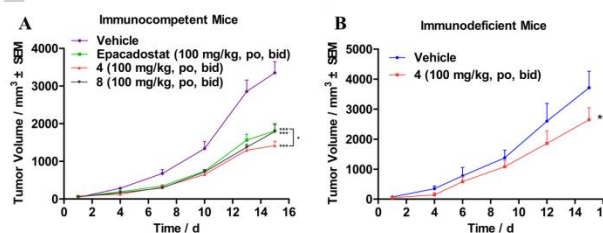


Figure 2. Compounds 4 and 8 effectively suppressed the tumor growth. (A) Antitumor efficacy of compounds 4 and 8 in murine CT-26 tumor allograft model. Data are expressed as the mean ± SEM (n = 6 mice/group). *** $P < 0.001$ compared with the control group; * $P < 0.05$ compared between group epacadostat and 4, determined with Student's *t* test. (B) *In vivo* efficacy of compound 4 in CT-26 tumor xenograft model. Data are expressed as the mean ± SEM (n = 6 mice/group). ** $P < 0.01$ compared with the control group, determined with Student's *t* test.

Overexpression of IDO1 is a common feature in many tumor types, which lead to Kyn production and accumulation and Trp degradation. Thus, to investigate the IDO1 activity *in vivo*, pharmacodynamic assay^[16] was performed. Wild-type female C57BL/6 mice were administrated orally with 4 (100 mg/kg) and then blood was collected at the indicated times. Blood samples were

analyzed by LC/MS/MS for Kyn level detection. As shown in Figure 3A, compound **4** significantly reduced plasma Kyn level after 0.5 h oral exposure and the effects maintained and enhanced in the next 8 h. Additionally, reduction of the tumor Kyn to Trp (Kyn/Trp) ratio caused by **4** and **8** was also measured in CT-26 tumor allograft model. Tumor samples were collected at 3 h after last dosing after 14 days of treatment (100 mg/kg, po, bid). The Kyn and Trp levels were determined by LC/MS/MS, and the ratios of Kyn/Trp were calculated. It was found that the Kyn/Trp ratio was significantly lower in compound **4** treated mice than that in the control (Figure 3B). The results indicated that compound **4** significantly inhibited IDO1 activity in tumor tissues and reduced Kyn level in plasma.

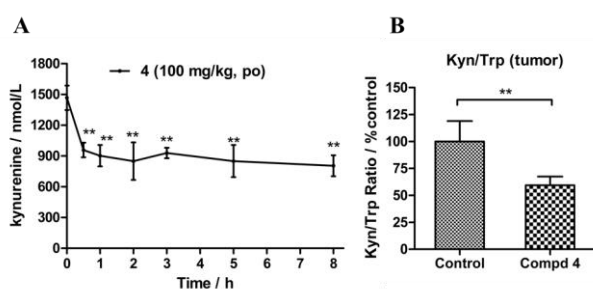


Figure 3. Compound **4** reduced Kyn and Kyn/Trp ratio efficiently. (A) Mean (\pm SD) plasma concentration-time profiles of Kyn in wild-type female C57BL/6 mice ($n = 3$) following po with **4** (100 mg/kg). (B) Mean (\pm SD) ratios of Kyn/Trp in CT-26 tumor allograft model. **, $P < 0.01$, determined with Student's t test.

In conclusion, we have demonstrated that single agents with the dual targeting capacity are a feasible and powerful tool to improve cancer immunotherapy, an emerging field in oncology. In these studies, hybrid molecules as IDO1/DNA dual-targeting agents are rationally designed, synthesized and evaluated. As the first-in-class example of such molecules, they exhibited significantly enhanced anticancer activity *in vitro* and *in vivo* with low toxicity. Among them, compound **4** showed the most potent IDO1 inhibitory activity ($IC_{50} = 0.13 \mu\text{M}$) and good cellular potency ($EC_{50} = 0.27 \mu\text{M}$), which significantly inhibits IDO1 activity in tumor tissues and reduces Kyn level in plasma. Importantly, it exhibits better *in vivo* antitumor efficacy than clinical candidate IDO1 inhibitor epacadostat (58.2% versus 47.5%, 100 mg/kg, po, bid) in the CT-26 allograft models without significant body weight loss and adverse effects. To the best of our knowledge, the study represents the first case of proof-of-concept of dual targeting strategy in emerging cancer immunotherapy. Systematic development of similar dual-targeting agents may create a general and fruitful approach to improving cancer immunotherapy.

Experimental Section

Molecular Modeling

Molecular modeling experiments were carried out with the Schrödinger Maestro 9.0 package. The crystal structure of IDO1 in complex with Amg-1 was obtained from protein database bank (PDB ID 4PK5)^[17] and

prepared for docking using Protein Preparation Wizard. During this process, waters were removed and hydrogens were added to the structure. The resulting structure was refined by OPLS3 force-field with the hydrogens only. Then, Receptor Grid Preparation was used to generate the protein grid for docking experiments. Amg-1 was picked for ligand identification. Fe in heme was selected which could participate in metal-ligand interactions. Other parameters were set default. Ligand Docking option was used for docking performance. Under Setting, SP (standard precision), "Dock flexibly", "Sample nitrogen inversions", "Sample ring conformation" and "Epik state penalties" to docking score were selected.

Conformations were generated and scored using glide score as fitness function. The best conformation was chosen to analyse the ligand-protein interaction.

IDO1 Enzyme Activity Assay^[18]

IDO1 catalyzes the oxidative cleavage of the pyrrole ring of the indole nucleus of tryptophan to yield NFK. The assays were performed at room temperature as described in the literature using 20 nM IDO1 (NOVUS Bioscience Inc. # H00003620-P01) and 2 mM D-Trp in the presence of 20 mM ascorbate, 3.5 μM methylene blue and 0.2 mg/mL catalase in 50 mM potassium phosphate buffer (pH 6.5). The initial reaction rates were recorded by continuously following the absorbance increase at 321 nm due to the formation of NFK. The IC_{50} values were calculated using nonlinear regression with normalized dose-response fit using Prism GraphPad software.

IDO1 Cellular Assay^[18]

HeLa cells were seeded in 96-well culture plates at a density of 6×10^3 per well. On the next day, human IFN- γ (Sangon Biotech # C600039, 50 ng/mL) and compounds in a total volume of 200 μL culture medium containing 15 $\mu\text{g}/\text{mL}$ of Trp were added to the cells. After incubation for 48 hours, 140 μL of the supernatant was mixed with 10 μL of 6.1N trichloroacetic acid and the mixture was incubated for 30 min at 50 $^{\circ}\text{C}$ to hydrolyze NFK produced by IDO1 to Kyn. The reaction mixture was then centrifuged for 10 minutes at 2500 rpm to remove sediments. 100 μL of the supernatant was mixed with 100 μL of 2% (w/v) p -dimethylaminobenzaldehyde in acetic acid and measured at 480 nm. The data was processed using nonlinear regression to generate EC_{50} values (Prism Graphpad).

In Vitro Cytotoxicity Assay

This assay was determined by the Cell Counting Kit-8 (CCK-8) method. Cells were plated in 96-well microtiter plates at a density of $6-10 \times 10^3/\text{well}$ and incubated in a humidified atmosphere with 5% CO_2 at 37 $^{\circ}\text{C}$ for 24 h. Test compounds were added onto triplicate wells with different concentrations and 0.1% DMSO for control. After they had been incubated for 48 h, 10 μL of the CCK-8 solution was added to each well and the plate was incubated for additional 1-4 h in the incubator. The absorbance (OD) was read on a WellsanMK-2 microplate reader (Labsystems) at 450 nm. The concentration causing 50% inhibition of cell growth (IC_{50}) was determined by the Logit method. All experiments were performed three times.

In Vitro Cell Apoptosis Assay

CT-26 (obtained from Shcellbank, $3 \times 10^5/\text{well}$) cells were incubated in six-well plates for 24 h, and then treated with 0.1% DMSO (as control), various concentrations of compounds **4** or **8** in fresh growth medium. After 48 h, the cells were then harvested by trypsinization and washed twice with cold PBS. After centrifugation and removal of the supernatants, cells were resuspended in 400 μL of 1 \times binding buffer, which was then added to 5 μL of annexin V-FITC and incubated at room

temperature for 15 min. After adding 10 μ L of PI, the cells were incubated at room temperature for another 15 min in the dark. The stained cells were analyzed by a flow cytometer (BD Accuri C6).

In Vitro Cell Cycle Assay

CT-26 (3×10^5 /well) cells were incubated in six-well plates (Corning) for 24 h, and then treated with 0.1% DMSO (as control), various concentrations of compounds **6** or **10** for 0-48 h. The treated cells were collected, resuspended, and incubated for 30 min at 37 °C with 25 μ g/mL PI and 10 μ g/mL RNase buffer. For each sample, at least 1×10^4 cells were analyzed using flow cytometry (BD Accuri C6).

In Vivo Antitumor Assay and Analysis of the Ratio of Kyn to Try in Tumor Tissues

Balb/c male mice or Balb/c nude male mice (certificate SCXK-2013-0016, weighing 18–20 g) were purchased from Shanghai Laboratory Animal Center, SLAC. The CT-26 colorectal cancer cells used for implantation were harvested during log phase growth and resuspended in phosphate-buffer saline. Each mice were inoculated s.c. into the right forelimb with 5×10^5 tumor cells. When tumor volumes approached ~ 50 mm³, the mice were assigned into groups randomly and treated orally with compound **4**, compound **8**, or epacadostat at doses 100 mg/kg twice every day, and the blank control group received an equal volume of water containing 0.5% carboxyl methyl cellulose and 0.5% Tween 80 twice every day. Compounds were reconstituted in 0.5% carboxyl methyl cellulose and 0.5% Tween 80 in water. Tumor volumes were monitored by caliper measurement of the length and width and calculated using the formula of $TV = \frac{1}{2} \times a \times b^2$, where *a* is the tumor length and *b* is the width. Tumor volumes and body weights were monitored every 4 days over the course of treatment. After 14 days of treatment, the mice were sacrificed and the tumor samples were collected at 3 h. The tumor samples were homogenized with 9 volumes (v/w) of PBS for 30 s. An aliquot of 12 μ L sample was added with 48 μ L PBS (pH7.4), mixed well, and the sample dilution factor is 5. Then added with 240 μ L IS (500 ng/mL) in MeOH-1%FA. The mixture was vortexed for 5 min and centrifuged at 5800 rpm for 10 min. Aliquots (50 μ L) of supernatant were diluted with aliquots (50 μ L) H₂O and then an aliquot of 2 μ L supernatant was injected onto the LC-MS/MS (API 6500) system. The levels of Kyn and Try were measured and the Kyn/Trp ratios were calculated.

In Vivo Pharmacodynamic Assay

Compound **4** at a dose of 100 mg/kg were administered by oral gavage to C57BL/6 male mice (certificate SCXK-2013-0018, *n* = 4 animals/group). Food will be removed for 2 h prior to study start and animals will be kept off food for the duration of the study. At various time points, mice were euthanized and blood was collected via retro-orbital puncture (under anesthesia with Isoflurane) into pre-cold EDTA-3K tubes. Blood sample was centrifuged at 4 °C (2000 g, 5 min) to obtain plasma within 15 min after sample collection. Then 60 μ L homogenized solution added with 240 μ L IS (500 ng/mL) in MeOH-1% trifluoroacetic acid. The mixture was vortexed for 5 min and centrifuged at 5800 rpm for 10 min. Aliquots (50 μ L) of supernatant were diluted with aliquots (50 μ L) H₂O and then an aliquot of 2 μ L supernatant was injected onto the LC-MS/MS (API 6500) system. The levels of Kyn were measured.

Synthesis

2-(4-(bis(2-chloroethyl)amino)phenyl)-N-(2-((4-(3-bromo-4-fluorophenyl)-5-oxo-4,5-dihydro-1,2,4-oxadiazol-3-yl)-1,2,5-oxadiazol-3-yl)amino)ethyl)acetamide (3e). A mixture of intermediate **1** (0.20 g, 0.4 mmol), intermediate **2e** (0.12 g, 0.4 mmol), HATU (0.16 g, 0.4 mmol), DIPEA (20 μ mol, 1 mmol) and DMF (10 mL) was stirred for 24 h at room temperature. The reaction was poured into ice/water (100 mL), and extracted with ethyl acetate (2 \times 100 mL). The combined organic

layers was washed with water, brine, dried over sodium sulfate, purified by column chromatography on SiO₂ (DCM: MeOH = 100: 1) to afford **3e** (0.15 g, 58%) as a white solid. ¹H NMR (DMSO-*d*₆, 600 MHz) δ : 8.09 (dd, *J* = 6.2, 2.5 Hz, 1H), 8.05 (t, *J* = 5.7 Hz, 1H), 7.71 (m, 1H), 7.60 (t, *J* = 8.5 Hz, 1H), 7.08 (d, *J* = 8.6 Hz, 2H), 6.67 (d, *J* = 8.6 Hz, 2H), 6.55 (t, *J* = 5.7 Hz, 1H), 3.70 (s, 8H), 3.31 (m, 4H), 3.23 (s, 2H).

The synthetic methods for intermediates **3a-3d** and **3f-3i** were similar to the synthesis of intermediate **3e**.

3-(4-((2-bis(2-hydroxyethyl)amino)ethyl)amino)-1,2,5-oxadiazol-3-yl)-4-(3-bromo-4-fluorophenyl)-1,2,4-oxadiazol-5(4H)-one (3j). Intermediate **1** (1.0 g, 2.0 mmol), water (75 mL) and acetic acid (25 mL) were added into a sealed tube in an ice water bath. Then ethylene oxide (3 mL) was slowly dropwise added with violent stirring. The mixture was further stirred for 24 h at room temperature. Then the pH value of the solution was adjusted to 7 by 2M NaOH aqueous solution. The aqueous phase was extracted with ethyl acetate (2 \times 100 mL). The combined organic layers was washed with water, brine, dried over sodium sulfate, purified by column chromatography on SiO₂ (DCM: MeOH = 100: 5) to afford **3j** (0.75 g, 78%) as a white solid. ¹H NMR (DMSO-*d*₆, 600 MHz) δ : 8.10 (dd, *J* = 6.2, 2.4 Hz, 1H), 7.74 (m, 1H), 7.61 (t, *J* = 8.5 Hz, 1H), 6.45 (s, 1H), 4.41 (s, 2H), 3.45 (s, 4H), 3.31 (s, 2H), 2.74 (s, 2H), 2.60 (s, 4H).

3-(4-((2-bis(2-chloroethyl)amino)ethyl)amino)-1,2,5-oxadiazol-3-yl)-4-(3-bromo-4-fluorophenyl)-1,2,4-oxadiazol-5(4H)-one (3k). Intermediate **3j** (0.5 g, 1.1 mmol) was dissolved in dichloromethane (40 mL). SOCl₂ (0.24 mL, 3.3 mmol) was added dropwise under the ice water bath. The reaction was stirred at 40 °C for 3 h. After cooling to room temperature, the mixture was concentrated in vacuo to give the desired product (0.46 g, 85 %) as a crude brown oil, which was used directly for the next step without further purification. ¹H NMR (DMSO-*d*₆, 600 MHz) δ : 8.09 (dd, *J* = 6.2, 2.6 Hz, 1H), 7.23 (m, 1H), 7.59 (t, *J* = 8.7 Hz, 1H), 6.36 (t, *J* = 5.8 Hz, 1H), 3.61 (t, *J* = 6.7 Hz, 4H), 3.30 (s, 2H), 2.90 (t, *J* = 6.9 Hz, 4H), 6.6 (t, *J* = 6.6 Hz, 2H).

3-(bis(2-chloroethyl)amino)-N-(2-((4-(N-(3-bromo-4-fluorophenyl)-N-hydroxycarbamimidoyl)-1,2,5-oxadiazol-3-yl)amino)ethyl)benzamide (4). A solution of intermediate **3a** (0.15 g, 0.2 mmol) in methanol (10 mL) was treated with 2 M NaOH (0.5 mL, 1.0 mmol) and stirred at 40 °C for 2 h. The reaction mixture was quenched with 6 N HCl to pH \sim 7 and the methanol was removed under reduced pressure. The solid that precipitated was filtered and washed with water to give the desired product (0.13 g, 93 %) as a white solid. ¹H NMR (DMSO-*d*₆, 600 MHz) δ : 11.41 (s, 1H), 8.84 (s, 1H), 8.50 (t, *J* = 5.6 Hz, 1H), 7.26 (t, *J* = 8.1 Hz, 1H), 7.12 (m, 4H), 6.88 (m, 1H), 6.74 (m, 1H), 6.30 (t, *J* = 6.0 Hz, 1H), 3.73 (m, 8H), 3.47 (m, 2H), 3.40 (m, 2H); ¹³C NMR (DMSO-*d*₆, 150 MHz) δ : 167.61, 156.20, 154.98, 153.40, 146.84, 140.45, 139.71, 138.49, 136.24, 129.80, 125.28, 121.92, 116.38, 116.09, 115.01, 110.88, 107.48, 52.39, 44.17, 41.51, 38.46; HRMS (ESI, positive) *m/z* calcd for C₂₂H₂₄BrCl₂FN₇O₃ (*M* + *H*): 604.0460, found 604.0463.

The synthetic methods for compounds **5-13** were similar to the synthesis of compound **4**.

2-(3-(bis(2-chloroethyl)amino)phenyl)-N-(2-((4-(N-(3-bromo-4-fluorophenyl)-N-hydroxycarbamimidoyl)-1,2,5-oxadiazol-3-yl)amino)ethyl)acetamide (5). White solid (0.12 g, 77%). ¹H NMR (DMSO-*d*₆, 600 MHz) δ : 11.47 (s, 1H), 8.88 (s, 1H), 8.15 (t, *J* = 5.0 Hz, 1H), 7.15 (t, *J* = 9.0 Hz, 1H), 7.10 (dd, *J* = 5.8, 2.7 Hz, 1H), 7.07 (t, *J* = 8.1 Hz, 1H), 6.74 (m, 1H), 6.61 (s, 1H), 6.56 (m, 2H), 6.24 (t, *J* = 5.7 Hz, 1H), 3.68 (s, 8H), 3.31 (s, 2H), 3.25 (m, 4H); ¹³C NMR (DMSO-*d*₆, 150 MHz) δ : 171.11, 156.07, 154.95, 153.36, 146.61, 140.37, 139.65, 138.43, 137.83, 129.69, 125.24, 121.90, 117.92, 116.36, 112.98, 110.36, 107.45, 52.55, 44.13, 43.29, 41.43, 37.95; ESI-MS (*m/s*): 618.27 [*M* + *H*].

3-(3-(bis(2-chloroethyl)amino)phenyl)-N-(2-((4-(N-(3-bromo-4-fluorophenyl)-N-hydroxycarbamimidoyl)-1,2,5-oxadiazol-3-

yl)amino)ethyl)propanamide (6). White solid (0.23 g, 85%). ¹H NMR (DMSO-*d*₆, 600 MHz) δ : 11.44 (s, 1H), 8.85 (s, 1H), 7.96 (s, 1H), 7.14 (t, *J* = 8.8 Hz, 1H), 7.10 (dd, *J* = 6.0, 2.7 Hz, 1H), 7.06 (t, *J* = 8.0 Hz, 1H), 6.76 (m, 1H), 6.54 (s, 1H), 6.50 (m, 2H), 6.20 (t, *J* = 5.6 Hz, 1H), 3.68 (s, 8H), 3.25 (s, 4H), 2.72 (t, *J* = 7.4 Hz, 2H), 2.48 (q, *J* = 1.7 Hz, 2H), 2.34 (t, *J* = 8.2 Hz, 2H); ¹³C NMR (DMSO-*d*₆, 150 MHz) δ : 172.36, 156.13, 154.99, 153.41, 146.77, 143.09, 140.43, 139.72, 138.51, 129.79, 125.28, 121.94, 117.28, 116.39, 112.20, 110.02, 107.51, 52.60, 44.22, 40.55, 41.58, 37.72, 31.99; ESI-MS (m/s): 632.27 [M + H].

4-(bis(2-chloroethyl)amino)-*N*-2-((4-(*N*-3-bromo-4-fluorophenyl)-*N*'-hydroxycarbamimidoyl)-1,2,5-oxadiazol-3-yl)amino)ethyl)benzamide (7). White solid (0.08 g, 64%). ¹H NMR (DMSO-*d*₆, 600 MHz) δ : 11.43 (s, 1H), 8.86 (s, 1H), 8.29 (t, *J* = 6.0 Hz, 1H), 7.71 (s, 1H), 7.70 (s, 1H), 7.13 (t, *J* = 8.3 Hz, 1H), 7.10 (dd, *J* = 6.0, 2.7 Hz, 1H), 6.77 (s, 1H), 6.75 (s, 1H), 6.73 (m, 1H), 6.29 (t, *J* = 6.0 Hz, 1H), 3.75 (m, 8H), 3.43 (t, *J* = 5.9 Hz, 2H), 3.37 (t, *J* = 5.8 Hz, 2H); ¹³C NMR (DMSO-*d*₆, 150 MHz) δ : 166.79, 156.18, 154.98, 153.39, 149.15, 140.47, 139.69, 138.51, 129.42, 125.27, 122.68, 121.91, 116.37, 111.33, 107.50, 52.27, 44.40, 41.48, 38.34; ESI-MS (m/s): 604.26 [M + H].

2-(4-(bis(2-chloroethyl)amino)phenyl)-*N*-2-((4-(*N*-3-bromo-4-fluorophenyl)-*N*'-hydroxycarbamimidoyl)-1,2,5-oxadiazol-3-yl)amino)ethyl)acetamide (8). White solid (0.16 g, 79%). ¹H NMR (DMSO-*d*₆, 600 MHz) δ : 11.46 (s, 1H), 8.86 (s, 1H), 8.04 (t, *J* = 5.6 Hz, 1H), 7.17 (t, *J* = 8.8 Hz, 1H), 7.13 (dd, *J* = 6.2, 2.6 Hz, 1H), 7.09 (s, 1H), 7.07 (s, 1H), 6.78 (m, 1H), 6.67 (s, 1H), 6.65 (s, 1H), 6.23 (t, *J* = 5.5 Hz, 1H), 3.69 (s, 8H), 3.28 (m, 6H); ¹³C NMR (DMSO-*d*₆, 150 MHz) δ : 171.56, 156.11, 154.99, 153.41, 145.31, 140.42, 139.73, 138.49, 130.44, 125.28, 124.88, 121.92, 116.40, 112.22, 107.52, 52.63, 44.19, 41.82, 41.59, 37.92; HRMS (ESI, positive) m/z calcd for C₂₃H₂₆BrCl₂FN₃O₃ (M + H): 618.0618, found 618.0614.

3-(4-(bis(2-chloroethyl)amino)phenyl)-*N*-2-((4-(*N*-3-bromo-4-fluorophenyl)-*N*'-hydroxycarbamimidoyl)-1,2,5-oxadiazol-3-yl)amino)ethyl)propanamide (9). White solid (0.11 g, 69%). ¹H NMR (DMSO-*d*₆, 600 MHz) δ : 11.46 (s, 1H), 8.88 (s, 1H), 7.96 (t, *J* = 5.1 Hz, 1H), 7.18 (t, *J* = 8.6 Hz, 1H), 7.13 (dd, *J* = 6.2, 2.8 Hz, 1H), 7.03 (s, 1H), 7.02 (s, 1H), 6.79 (m, 1H), 6.65 (s, 1H), 6.64 (s, 1H), 6.23 (t, *J* = 5.4 Hz, 1H), 3.69 (s, 8H), 3.27 (m, 4H), 2.69 (t, *J* = 7.2 Hz, 2H), 2.31 (t, *J* = 8.1 Hz, 2H); ¹³C NMR (DMSO-*d*₆, 150 MHz) δ : 172.44, 156.13, 155.10, 153.39, 144.95, 140.42, 139.71, 138.51, 129.95, 129.63, 125.27, 121.93, 116.40, 112.34, 107.53, 52.66, 44.26, 41.61, 37.97, 37.74, 30.56; ESI-MS (m/s): 632.27 [M + H].

4-(4-(bis(2-chloroethyl)amino)phenyl)-*N*-2-((4-(*N*-3-bromo-4-fluorophenyl)-*N*'-hydroxycarbamimidoyl)-1,2,5-oxadiazol-3-yl)amino)ethyl)butanamide (10). White solid (0.04 g, 71%). ¹H NMR (DMSO-*d*₆, 600 MHz) δ : 11.48 (s, 1H), 8.90 (s, 1H), 7.94 (s, 1H), 7.15 (t, *J* = 8.5 Hz, 1H), 7.10 (m, 1H), 7.00 (d, *J* = 7.7 Hz, 2H), 6.75 (m, 1H), 6.63 (d, *J* = 8.5 Hz, 2H), 6.23 (s, 1H), 3.68 (s, 8H), 3.27 (s, 4H), 2.41 (t, *J* = 7.1 Hz, 2H), 2.06 (t, *J* = 7.1 Hz, 2H), 1.72 (m, 2H); ¹³C NMR (DMSO-*d*₆, 150 MHz) δ : 172.84, 156.12, 154.96, 153.38, 144.85, 140.38, 139.70, 138.49, 130.38, 129.75, 125.24, 121.89, 116.44, 112.34, 107.49, 52.69, 44.32, 41.61, 37.74, 35.31, 34.05, 27.67; HRMS (ESI, positive) m/z calcd for C₂₅H₃₀BrCl₂FN₃O₃ (M + H): 646.0925; found 646.0929.

2-amino-3-(4-(bis(2-chloroethyl)amino)phenyl)-*N*-2-((4-(*N*-3-bromo-4-fluorophenyl)-*N*'-hydroxycarbamimidoyl)-1,2,5-oxadiazol-3-yl)amino)ethyl)propanamide (11). White solid (0.02 g, 54%). ¹H NMR (CD₃OD-*d*₆, 600 MHz) δ : 7.12 (dd, *J* = 6.0, 2.6 Hz, 1H), 7.07 (s, 1H), 7.06 (s, 1H), 7.02 (t, *J* = 8.6 Hz, 1H), 6.84 (m, 1H), 6.64 (s, 1H), 6.62 (s, 1H), 3.70 (t, *J* = 7.3 Hz, 4H), 3.62 (t, *J* = 6.7 Hz, 4H), 3.50 (t, *J* = 7.1 Hz, 1H), 3.43 (m, 2H), 3.27 (m, 2H), 2.85 (dd, *J* = 13.4, 6.5 Hz, 1H), 2.75 (dd, *J* = 13.7, 7 Hz, 1H); HRMS (ESI, positive) m/z calcd for C₂₄H₂₉BrCl₂FN₃O₃ (M + H): 647.3393 found 647.0894.

4-(5-(bis(2-chloroethyl)amino)-1-methyl-1*H*-benzo[d]imidazol-2-yl)-*N*-2-((4-(*N*-3-bromo-4-fluorophenyl)-*N*'-hydroxycarbamimidoyl)-1,2,5-oxadiazol-3-yl)amino)ethyl)butanamide (12). White solid (0.03 g, 66%). ¹H NMR (DMSO-*d*₆, 600 MHz) δ : 11.90 (s, 1H), 8.87 (s, 1H), 7.98 (s, 1H), 7.32 (d, *J* = 8.9 Hz, 1H), 7.14 (t, *J* = 8.9 Hz, 1H), 7.09 (m, 1H), 6.87 (d, *J* = 2.5 Hz, 1H), 6.76 (m, 2H), 6.20 (s, 1H), 3.68 (s, 8H), 3.65 (s, 3H), 3.26 (m, 4H), 2.80 (t, *J* = 7.5 Hz, 2H), 2.20 (t, *J* = 7.5 Hz, 2H), 1.97 (t, *J* = 7.5 Hz, 2H); ¹³C NMR (DMSO-*d*₆, 150 MHz) δ : 172.66, 156.10, 155.12, 154.96, 153.37, 142.93, 140.45, 139.74, 138.53, 125.22, 121.88, 116.37, 110.73, 107.49, 102.41, 53.90, 44.23, 41.88, 37.68, 35.10, 29.98, 26.37, 23.47; ESI-MS (m/s): 700.29 [M + H].

4-((2-(bis(2-chloroethyl)amino)ethyl)amino)-*N*-(3-bromo-4-fluorophenyl)-*N*'-hydroxy-1,2,5-oxadiazole-3-carboximidamide (13). Light yellow solid (0.23 g, 74%). ¹H NMR (DMSO-*d*₆, 600 MHz) δ : 11.40 (s, 1H), 8.83 (s, 1H), 7.16 (t, *J* = 8.7 Hz, 1H), 7.07 (dd, *J* = 6.0, 2.5 Hz, 1H), 6.74 (m, 1H), 6.14 (t, *J* = 5.6 Hz, 1H), 3.60 (t, *J* = 6.8 Hz, 4H), 3.24 (q, *J* = 6.0 Hz, 2H), 2.88 (t, *J* = 6.8 Hz, 4H), 2.76 (t, *J* = 6.8 Hz, 2H); ¹³C NMR (DMSO-*d*₆, 150 MHz) δ : 155.57, 154.49, 152.90, 139.92, 139.22, 138.05, 124.70, 121.31, 107.05, 55.49, 51.76, 42.29, 42.05; MS (ESI, positive) m/z calcd for C₁₅H₁₇BrCl₂FN₃O₂ (M - H): 482.9936; found 482.9941.

Acknowledgements

This work was supported by the National Key R&D Program of China (2017YFA0506000 to C. S.), National Natural Science Foundation of China (21738002 to W. W and C. S and 81725020 to C. S.).

Conflict of interest

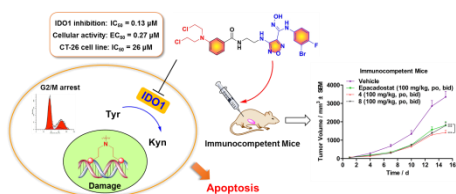
The authors declare no conflict of interest.

Keywords: Cancer immunotherapy • IDO1 • Multi-targeting drug design • Antitumor activity

- [1] P. Sharma, J. P. Allison, *Science* **2015**, *348*, 56-61.
- [2] J. A. Joyce, D. T. Fearon, *Science* **2015**, *348*, 74-80.
- [3] a) T. Boon, P. van der Bruggen, *J Exp Med* **1996**, *183*, 725-729; b) R. D. Schreiber, L. J. Old, M. J. Smyth, *Science* **2011**, *331*, 1565-1570.
- [4] A. B. Dounay, J. B. Tuttle, P. R. Verhoest, *J Med Chem* **2015**, *58*, 8762-8782.
- [5] C. J. Austin, L. M. Rendina, *Drug Discov Today* **2015**, *20*, 609-617.
- [6] T. Jiang, Y. Sun, Z. Yin, S. Feng, L. Sun, Z. Li, *Future Med Chem* **2015**, *7*, 185-201.
- [7] Y. W. Moon, J. Hajjar, P. Hwu, A. Naing, *J Immunother Cancer* **2015**, *3*, 51.
- [8] a) R. Metz, S. Rust, J. B. Duhadaway, M. R. Mautino, D. H. Munn, N. N. Vahanian, C. J. Link, G. C. Prendergast, *Oncoimmunology* **2012**, *1*, 1460-1468; b) H. K. Koblish, M. J. Hansbury, K. J. Bowman, G. Yang, C. L. Neilan, P. J. Haley, T. C. Burn, P. Waeltz, R. B. Sparks, E. W. Yue, A. P. Combs, P. A. Scherle, K. Vaddi, J. S. Fridman, *Mol Cancer Ther* **2010**, *9*, 489-498; c) S. Qian, M. Zhang, Q. Chen, Y. He, W. Wang, Z. Wang, *RSC Advances* **2016**, *6*, 7575-7581.
- [9] S. Yang, X. Li, F. Hu, Y. Li, Y. Yang, J. Yan, C. Kuang, Q. Yang, *J Med Chem* **2013**, *56*, 8321-8331.
- [10] D. H. Munn, A. L. Mellor, *Trends Immunol* **2016**, *37*, 193-207.
- [11] a) A. J. Muller, J. B. DuHadaway, P. S. Donover, E. Sutanto-Ward, G. C. Prendergast, *Nat Med* **2005**, *11*, 312-319; b) D. Y. Hou, A. J. Muller, M. D. Sharma, J. DuHadaway, T. Banerjee, M. Johnson, A. L. Mellor, G. C. Prendergast, D. H. Munn, *Cancer Res* **2007**, *67*, 792-801; c) M. Li, A. R. Bolduc, M. N. Hoda, D. N. Gamber, S. B. Dolisca, A. K. Bolduc, K.

- Hoang, C. Ashley, D. McCall, A. M. Rojjani, B. L. Maria, O. Rixe, T. J. MacDonald, P. S. Heeger, A. L. Mellor, D. H. Munn, T. S. Johnson, *J Immunother Cancer* **2014**, *2*, 21.
- [12] S. R. Selvan, J. P. Dowling, W. K. Kelly, J. Lin, *Curr Cancer Drug Targets* **2016**, *16*, 755-764.
- [13] S. R. R. And, R. M. Williams, *Chemical Reviews* **1998**, *98*, 2723-2796.
- [14] a) L. F. Povirk, D. E. Shuker, *Mutat Res* **1994**, *318*, 205-226; b) W. U. Knauf, T. Lissitchkov, A. Aldaoud, A. M. Liberati, J. Loscertales, R. Herbrecht, G. Juliusson, G. Postner, L. Gercheva, S. Goranov, M. Becker, H. J. Fricke, F. Huguet, I. Del Giudice, P. Klein, K. Merkle, M. Montillo, *Br J Haematol* **2012**, *159*, 67-77.
- [15] S. Tojo, T. Kohno, T. Tanaka, S. Kamioka, Y. Ota, T. Ishii, K. Kamimoto, S. Asano, Y. Isobe, *ACS Med Chem Lett* **2014**, *5*, 1119-1123.
- [16] E. W. Yue, R. Sparks, P. Polam, D. Modi, B. Douty, B. Wayland, B. Glass, A. Takvorian, J. Glenn, W. Zhu, M. Bower, X. Liu, L. Leffert, Q. Wang, K. J. Bowman, M. J. Hansbury, M. Wei, Y. Li, R. Wynn, T. C. Burn, H. K. Koblisch, J. S. Fridman, T. Emm, P. A. Scherle, B. Metcalf, A. P. Combs, *ACS Med Chem Lett* **2017**, *8*, 486-491.
- [17] S. Tojo, T. Kohno, T. Tanaka, S. Kamioka, Y. Ota, T. Ishii, K. Kamimoto, S. Asano, Y. Isobe, *ACS Med Chem Lett* **2014**, *5*, 1119-1123.
- [18] M. F. Cheng, M. S. Hung, J. S. Song, S. Y. Lin, F. Y. Liao, M. H. Wu, W. Hsiao, C. L. Hsieh, J. S. Wu, Y. S. Chao, *Bioorganic & Medicinal Chemistry Letters* **2014**, *24*, 3403-3406.

Entry for the Table of Contents



Kill two birds with one stone. The first-in-class IDO1-DNA dual targeting inhibitors were designed to improve the efficacy of small molecule cancer immunotherapy.